PHYSICAL REVIEW B **78**, 140102(R) (2008)

Synchrotron x-ray scattering evidence for interlayer structural coupling in $(PbMg_{1/3}Nb_{2/3}O_3)_{(1-x)\Lambda}/(PbTiO_3)_{x\Lambda}$ superlattices

N. Lemée,[1,*] E. Dooryhée,[2] H. Bouyanfif,[1] F. Le Marrec,[1] M. Nemoz,[2,†] J. L. Hodeau,[2] and M. G. Karkut[1]
[1]*LPMC, Université de Picardie Jules Verne, 33 rue St. Leu, 80039 Amiens, France*
[2]*Institut Néel, CNRS-UJF, UPR 2940, 25 avenue des Martyrs, BP 166, 38042 Grenoble, France*
(Received 7 July 2008; revised manuscript received 19 September 2008; published 10 October 2008)

We present evidence for in-plane coupling in relaxor $PbMg_{1/3}Nb_{2/3}O_3$ / ferroelectric $PbTiO_3$ superlattices $[PMN_{(1-x)\Lambda}/PT_{x\Lambda}]_{10}$. For constant superlattice wavelength $\Lambda=d_{PMN}+d_{PT}$, we find that by varying the constituents thicknesses d_{PMN} and d_{PT} a significant effect is observed on the internal a_1/a_2 domain structure of the PT layers as well as on the appearance of domains in PMN. Since the strain effects on the structural patterns can be modulated by adjusting x, this is one way to control the polarization axis on a nanoscale level.

DOI: 10.1103/PhysRevB.78.140102 PACS number(s): 77.84.−s, 61.05.cp, 68.65.Cd, 77.80.Dj

Because of their technological potential and underlying fundamental issues, significant effort, both theoretical and experimental, is currently devoted to studying the effects of size and strain in ferroelectric perovskite thin films and superlattices (SLs). Much of this work exploits $PbTiO_3$ (PT) since it is a well-known ferroelectric which has been widely studied[1–7,31] and whose large bulk tetragonality $c/a=1.065$ leads to a characteristic domain structure. In addition, several theoretical approaches have been devoted to heteroepitaxial ferroelectric thin films[8–13] and, more recently, to ferroelectric superlattices.[14–16] Temperature dependent domain stability maps have been established as a function of the lattice mismatch between the film and the single-crystal substrate. These results on single domain PT thin films and superlattices show that as the misfit strain goes from compressive to tensile, the domain structure varies from a purely tetragonal c phase (c is the polar axis), to a monoclinic r phase [the polarization is tilted in the (110) plane], and finally to an orthorhombic aa-domain pattern (the polarization is along the [110] direction). In polydomain PT thin films,[9,10] the dependence on misfit strain is characterized by a change in the domain structure from purely c domain, to mixed c and a domains, and to the a_1/a_2 pattern. In the $a_1/a_2/a_1/a_2$ arrangement, the a_1 domains are oriented such that the c axis is aligned along the [100] direction of the substrate, while in the a_2 domains c is along the [100] direction of the substrate; the a_1 and a_2 domains have a 90° rotational relationship between each other about the substrate normal. Generally the experimentally observed domain structures in PT films are reported to be purely c domains or mixed c and a domains.[1–4,17–20] Recently, ultrathin (60 Å) PT films were shown to exhibit an r- and ac-domain pattern, the polarization being tilted in the (010) plane.[2]

Most studies on PT thin films report the behavior of the out-of-plane or c-axis polarization. In c-oriented thin films, in particular, a decrease in tetragonality and polarization with decreasing film thickness was measured and explained by imperfect screening of the depolarizing field.[1] The effect of the biaxial strains on the polarization axis when it lies in the plane of the film, has not yet, to our knowledge, been investigated. We now present a study of strain effects in ferroelectric SLs based on PT. We recently reported the results of an x-ray diffraction and Raman spectroscopy study on a series of $PMN_{(1-x)\Lambda}/PT_{x\Lambda}$ SLs grown by pulsed laser deposition on single-crystal MgO buffered with the conducting oxide $La_{0.5}Sr_{0.5}CoO_3$ (LSCO).[21–23] We showed that the polarization of the PT layers in these SLs entirely lies in the plane of the film.[22,23] Some features of these samples are reported in Table I. It is therefore possible to study the effect of biaxial strain on the in-plane polar axis in such SL structures. In SLs, the strains are periodically applied to the top and bottom interfaces of the individual layers and the relevant mismatch parameter is between the two constituents: the substrate, as we shall demonstrate, plays a secondary role.

In our $PMN_{(1-x)\Lambda}/PT_{x\Lambda}$ SLs, tensile epitaxial strains are imposed upon the PT layers by the adjacent PMN layers (bulk PMN is cubic, with $a_{bulk}=4.049$ Å). The PMN layers are in turn compressively strained by the adjacent PT layers. Moreover, since the periodicity Λ is kept approximately constant (130–150 Å) for all samples, this strain effect can be modified depending on the PT/PMN thickness ratio in the period. In these SLs, the stress in the PT layers can be as high as 3.6 GPa as estimated by Raman measurements.[23] The strain induced in these structures stabilizes the ferroelectric phase in the PT layers, at least up to 873 K, well above the bulk T_c of 765 K. The purpose of this Rapid Communication is to analyze the in-plane structure of the SL constituents as their relative composition x is varied within each modulation period. Measurements were performed at the French CRG BM2 beamline at the European Synchrotron Radiation (ESRF). Reciprocal space maps (RSMs) over the (H0L) and (0KL) nodes were obtained by determining the orientation matrix of each sample in the frame of the substrate, which acts as an internal unstrained standard. The experiments were carried out in asymmetric reflection, using a monochromatic beam of 9.865 keV ($\lambda=1.2568$ Å). The RSMs presented here are plotted in the reciprocal-lattice units of the substrate.

Using both standard θ-2θ x-ray diffraction[23] and (00L) reciprocal space mapping, we observe satellite peaks for all the superlattices presented in this study. These satellite peaks are characteristic of a modulated structure along the growth direction and are representative of the entire series of $PMN_{(1-x)\Lambda}/PT_{x\Lambda}$ SLs. In Fig. 1 we compare the (024) RSMs for two extreme compositions: $x=0.2$ and $x=0.8$, one rich in PMN and the other one rich in PT. The two RSMs are strikingly different: at $L=4.3$, only a single peak is present for the

TABLE I. List of superlattices, whose periodicity Λ and layer thicknesses in the period (t_{PMN} and t_{PT}) are estimated from θ-2θ x-ray diffractograms reported in Ref. 21.

	$PMN_{(1-x)\Lambda}/PT_{x\Lambda}$				
x	0.1	0.2	0.35	0.5	0.8
Periodicity Λ(Å)	130	130	140	150	150
t_{PMN}(Å)	117	104	91	75	30
t_{PT}(Å)	13	26	49	75	120

$PMN_{0.8\Lambda}/PT_{0.2\Lambda}$ [Fig. 1(a)] whereas a double peak structure occurs for the $PMN_{0.2\Lambda}/PT_{0.8\Lambda}$ at the same L value [Fig. 1(b)]. This clearly demonstrates a strong compositional dependence of the in-plane structure of these SLs, at constant modulation periodicity. The features present in the (024) RSMs (Fig. 1) are also observed in the (204) RSMs (not shown) for both samples. This means that the in-plane symmetry remains unchanged by a rotation of 90° about the sample normal. Therefore, the structure is consistent with a quadratic in-plane symmetry.

For the $PMN_{0.8\Lambda}/PT_{0.2\Lambda}$ sample [Fig. 1(a)], no a_1/a_2 domain structure is detected in the PT layers. Along the [001] direction, the reflections of the thin PT layers are strictly aligned with the reflections of the thick PMN layers. Thus, in the PMN-rich SL, the in-plane strains that the thick PMN layers impose on the thin PT layers are sufficiently strong so as to almost suppress the a_1/a_2 domain structure of PT. The PT layers are forced to nearly adopt the square in-plane structure possessed by the PMN layers. For the $PMN_{0.2\Lambda}/PT_{0.8\Lambda}$ sample [Fig. 1(b)], an a_1/a_2 domain structure is clearly discernible. The splitting of the PT reflection in Fig. 1(b) for this sample is unchanged by a 90° rotation about the sample normal. This also is characteristic of an a_1/a_2 domain structure. The one-dimensional (1D) cross sections of the PMN diffraction along ⟨010⟩ are shown in Fig. 1(c) for three distinct L values: at L=4.19, a superlattice local maximum, at L=4.21, a superlattice local minimum, and at L=4.23, another superlattice local maximum. We observe a weak splitting on the SL maxima. Even if the splitting from the PMN layers is much less pronounced than that from the PT layers (x-ray scattering is intrinsically weaker from PMN than from PT) these results suggest the presence of an a_1/a_2 domain structure in normally domain-free PMN. Therefore, PT imposes its in-plane a_1/a_2 domain pattern on the adjacent PMN layers at high x. This has, to our knowledge, never been previously observed in pseudocubic bulk or thin-film relaxor materials. The fact that the PMN and PT layers in these two different SL samples adopt strikingly different structures highlights the in-plane structural coupling that can take place in superlattice systems. In SLs such changes in symmetry induced by interfacial strain and controlled by the periodicity have been observed for example in the $SrTiO_3$ layer in $BaTiO_3/SrTiO_3$ SLs.[24] To quantify more precisely the effect of the compositional in-plane coupling on the tetragonality in the ferroelectric PT layers, we have examined the (042) reflection in reciprocal space for all five SLs listed in Table I. Due to this split distribution of the

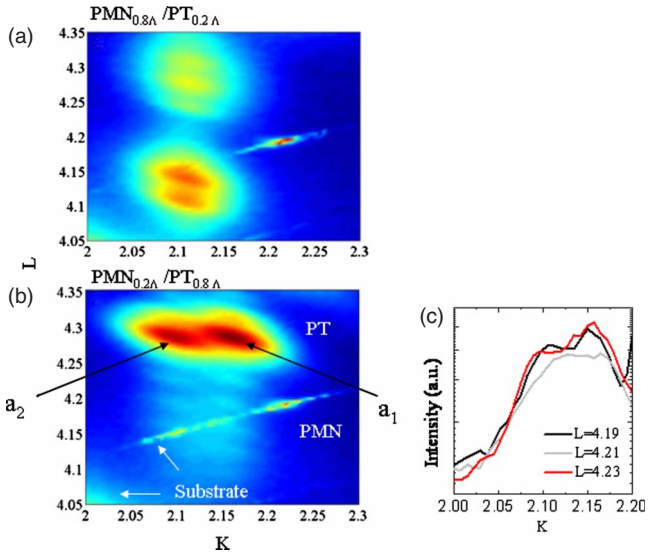

FIG. 1. (Color online) (Left) Logarithmic (0KL) reciprocal space maps around the 024 reflection for (a) $PMN_{0.8\Lambda}/PT_{0.2\Lambda}$ and (b) $PMN_{0.2\Lambda}/PT_{0.8\Lambda}$. The streaks diagonally crossing the maps are from the substrate. (Right) The corresponding 1D transversal cross sections for $PMN_{0.2\Lambda}/PT_{0.8\Lambda}$, at three L values (L=4.19, 4.21,4.23), are reported; (c) the disappearance of the splitting and the decrease in intensity at L=4.21 are in agreement with the presence of an a_1/a_2 domain structure in PT and PMN layers.

scattering intensity of PT along [010] in the (0KL) maps, we can simultaneously measure the value $a_{\parallel}$ of the a-lattice parameter of the a_1 domains and the value $c_{\parallel}$ of the c- (polar) lattice parameter of the a_2 domains.[25] The RSM maps for the entire series of constant Λ SLs are presented in Fig. 2 as well as the corresponding 1D cross sections of the PT reflections along the ⟨010⟩ direction.[26] With decreasing x (from bottom to top in Fig. 2), as the thickness of the PT layers decreases (or as the PMN thickness increases) the reflection from the a_1 domains gradually approaches that of the a_2 domains, meaning that the value $a_{\parallel}$ of the nonpolar a axis tends toward the value $c_{\parallel}$ of the in-plane polar c axis. Hence the tetragonality c/a decreases from 1.033 to 1.015 as x decreases from 0.8 to 0.1. These PT c/a values are notably smaller than c/a=1.065 in bulk PT. The c/a ratios in our SLs are comparable and even smaller than the smallest c/a values (1.03) reported in the literature for c-oriented PT thin films.[1] Figure 3 displays the in- and out-of-plane lattice parameters as a function of the (a) PT layer thickness, and as a function of the (b) PMN layer thickness. The in-plane polar c axis of the PT layers ($c_{\parallel}$) is found to be nearly constant and close to 4.05 Å, which is significantly smaller than the bulk value 4.153 Å. This very low value also contributes to the small c/a ratio in the PT layers. Furthermore, as can be clearly seen in Fig. 2(left), the position of the a_2 reflection is almost aligned with the PMN reflection for all compositions; it appears as if the polar axis lattice parameter has adjusted itself to that of the PMN lattice parameter (see Fig. 3). As x decreases, we observe an increase in the in-plane a-axis value ($a_{\parallel}$), which eventually tends toward the in-plane c axis value ($c_{\parallel}$). This is the result of a strengthening of the in-plane tensile strain which the PMN layers impose upon the PT layers.

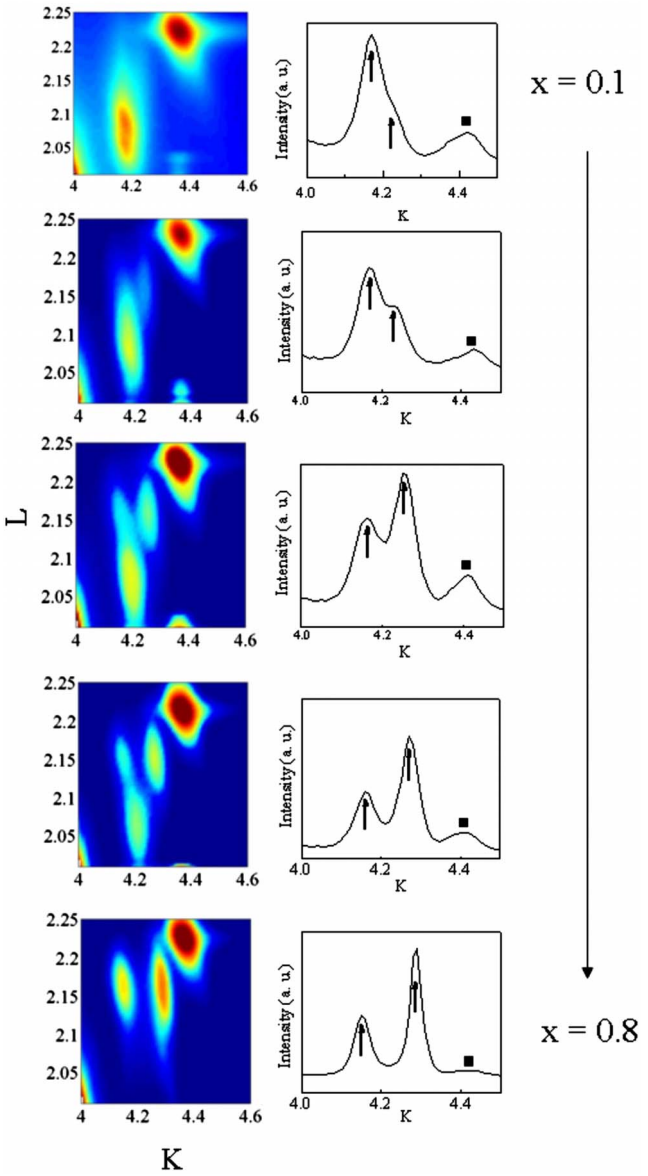

FIG. 2. (Color online) Logarithmic (0KL) reciprocal space maps about the 042 reflection of $PMN_{(1-x)\Lambda}$-$PT_{x\Lambda}$ and the corresponding linear scale transversal cross sections on PT layer reflections along the ⟨010⟩ direction (L=2.15) from x=0.1 (top figure) to 0.8 (bottom figure). The arrows indicate the splitting related to the a_1/a_2 domains, and the squares indicate the reflection related to the LSCO buffer layer. The intense reflection at (0, 4.4, 2.225) is from the LSCO buffer layer.

As the $c_{\|}$ value is almost similar to that of the in-plane lattice parameter of PMN, there is no significant effect on its value and the entire variation in the tetragonality is taken up by a change in the in-plane a-axis value. Hence, the thickness of the individual layers controls the structure of the SLs. There have been experimental and theoretical reports[15,27,28] on the effects of the relative thickness of SL layers via polarization-strain coupling. Nevertheless, in such systems, the 180° domain patterns configuration with out-of-plane polarization is substantially different from the PMN/PT SLs described here, making a direct comparison of the results problematic. In fact, since the polarization lies in the film plane in our SLs,

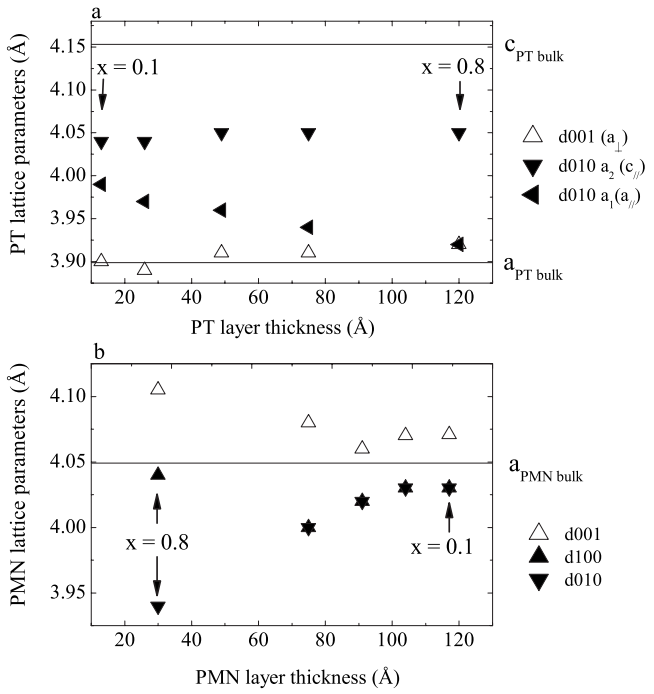

FIG. 3. Evolution of the in-plane (filled triangles) and out-of-plane (open triangles) lattice parameters, extracted from the RSM maps and from the (00L) x-ray diffraction longitudinal scans, as a function of layer thickness for (a) PT layers and for (b) PMN layers. Note that the "stars" in (b) are the results of overlap of d_{010} and d_{100} in PMN. For comparison, the lattice parameters of the bulk are listed here and indicated by solid lines in the figure: PT (tetragonal, a=3.899 Å, c=4.153 Å) and PMN (cubic, a=4.049 Å).

electrostatic energy is not really a factor in domain formation. The influence of the thickness of the layers PMN/PT SLs on the domain patterns reported here results primarily from elastic interactions.

Finally, the out-of-plane lattice parameters provided in Fig. 3 were determined from (00L) x-ray diffraction scans (not shown here) at 0.7758 Å over several orders (from L =1 to 8). By modeling these diffraction profiles using the program MULATRE (multilattice refinement),[29,30] we accurately extract the mean out-of-plane lattice parameter d_{001} of the PMN and that of the PT layers for all superlattices. For all SL compositions, the d_{001} a-axis values of the PT layers are comparable. Therefore the strain in the PT layers does not significantly change, as one would have intuitively anticipated when the PT thickness goes from 120 to 13 Å. However, this insensitivity of the out-of-plane nonpolar a axis under in-plane biaxial stress is consistent with hydrostatic pressure measurements on bulk PT reported by Nelmes and Katrusiak.[31] They show that, while there is a strong polar c-axis dependence as a function of applied pressure up to 6.35 GPa, the a axis remains relatively constant over this pressure range. As the thickness of the PT layers increases in the SL modulation period, the PT structure progressively changes from orthorhombic to tetragonal without modification of the polar axis but only with the relaxation of the in-plane a-lattice parameter. In the PMN layers, the structure remains tetragonal and unchanged for a layer thickness between 75 and 117 Å). The d_{100} and d_{010} values are equal and

close to the value $c_{\parallel}$ of the c lattice parameter of PT. The PMN lattice parameters are compressively strained in plane which induces a tetragonal structure in these layers that is far from the pseudocubic symmetry of bulk PMN. The coupling between the in-plane structures of the relaxor and the ferroelectric is strongest in the $PMN_{0.2\Lambda}/PT_{0.8\Lambda}$ SL, since we observe evidence for an a_1/a_2 domainlike structure. An in-plane distortion of about 1.02 is determined in these PMN layers. This is very close to the value of 1.033 measured for the PT layers in this SL and, consequently, its symmetry is unambiguously orthorhombic.

In conclusion, interlayer structural coupling has been induced between the relaxor PMN and the ferroelectric PT in PMN/PT superlattices by adjusting the PMN to PT thickness ratio in the period. The effects of strains in such superlattices generate structural patterns in these materials that are not ordinarily achievable in thin films, and can also provide a means to control the polarization direction in very thin ferroelectric layers.

ACKNOWLEDGMENTS

We thank N. Boudet and J. F. Bérar for technical assistance during the synchrotron experiments. This work was partially supported by an E. U. STREP MULTICERAL (Contract No. FP-6-NMP-CT-2006-032616).

*Corresponding author; nathalie.lemee@u-picardie.fr

†Present address: CRHEA, rue B. Grégory, 06560 Valbonne, France

[1] C. Lichtensteiger, J. M. Triscone, J. Junquera, and P. Ghosez, Phys. Rev. Lett. **94**, 047603 (2005).

[2] G. Catalan, A. Janssens, G. Rispens, S. Csiszar, O. Seeck, G. Rijnders, D. H. A. Blank, and B. Noheda, Phys. Rev. Lett. **96**, 127602 (2006).

[3] A. H. G. Vlooswijk, B. Noheda, G. Catalan, A. Janssens, B. Barcones, G. Rijnders, D. H. A. Blank, S. Venkatesan, B. Kooi, and J. T. M. de Hosson, Appl. Phys. Lett. **91**, 112901 (2007).

[4] P. E. Janolin, F. Le Marrec, J. Chevreul, and B. Dkhil, Appl. Phys. Lett. **90**, 192910 (2007).

[5] S. P. Alpay and A. L. Roytburd, J. Appl. Phys. **83**, 4714 (1998).

[6] A. L. Roytburd and Y. Yu, Ferroelectrics **144**, 137 (1993).

[7] C. M. Foster, Z. Li, M. Buckett, D. Miller, P. M. Baldo, L. Rehn, G. R. Bai, D. Guo, H. You, and K. L. Merkle, J. Appl. Phys. **78**, 2607 (1995).

[8] N. A. Pertsev, A. G. Zembilgotov, and A. K. Tagantsev, Phys. Rev. Lett. **80**, 1988 (1998).

[9] N. A. Pertsev and V. G. Koukhar, Phys. Rev. Lett. **84**, 3722 (2000).

[10] V. G. Koukhar, N. A. Pertsev, and R. Waser, Phys. Rev. B **64**, 214103 (2001).

[11] A. E. Romanov, W. Pompe, and J. S. Speck, J. Appl. Phys. **79**, 4037 (1996).

[12] J. S. Speck and W. Pompe, J. Appl. Phys. **76**, 466 (1994).

[13] J. S. Speck, A. C. Daykhin, A. Seifert, A. E. Romanov, and W. Pompe, J. Appl. Phys. **78**, 1696 (1995).

[14] F. A. Urtiev, V. G. Kukhar, and N. A. Pertsev, Appl. Phys. Lett. **90**, 252910 (2007).

[15] M. Dawber, C. Lichtensteiger, M. Cantoni, M. Veithen, P. Ghosez, K. Johnston, K. M. Rabe, and J. M. Triscone, Phys. Rev. Lett. **95**, 177601 (2005).

[16] E. Bousquet, M. Dawber, N. Stucki, C. Lichtensteiger, P. Hermet, S. Gariglio, J. M. Triscone, and P. Ghosez, Nature (London) **452**, 732 (2008).

[17] K. S. Lee, J. H. Choi, J. Y. Lee, and S. Baik, J. Appl. Phys. **90**, 4095 (2001).

[18] Z. Li, C. M. Foster, D. Guo, H. Zhang, G. R. Bai, P. M. Baldo, and L. E. Rehn, Appl. Phys. Lett. **65**, 1106 (1994).

[19] K. S. Lee and S. Baik, J. Appl. Phys. **87**, 8035 (2000).

[20] Y. K. Kim, K. Lee, and S. Baik, J. Appl. Phys. **95**, 236 (2004).

[21] H. Bouyanfif, N. Lemée, M. El Marssi, F. Le Marrec, B. Dkhil, J. Chevreul, B. Fraisse, J. C. Picot, and M. G. Karkut, Phys. Rev. B **76**, 014124 (2007).

[22] H. Bouyanfif, N. Lemée, M. El Marssi, F. Le Marrec, B. Dkhil, and M. G. Karkut, Ferroelectrics **316**, 131 (2005).

[23] H. Bouyanfif, M. El Marssi, N. Lemée, F. Le Marrec, M. G. Karkut, and B. Dkhil, Phys. Rev. B **71**, 020103(R) (2005).

[24] S. Ríos, A. Ruediger, A. Q. Jiang, J. F. Scott, H. Lu, and Z. Chen, J. Phys.: Condens. Matter **15**, L305 (2003).

[25] Working about the (042) reflection provides better accuracy compared to the (024) reflection for determining the in-plane lattice parameters of the PT layers. This is so because the increase in the K value leads to a wider separation between the a_1 and a_2 reflections. Unfortunately the counterpart is that the intensity of this reflection is lower than that from the (024) reflection of the PMN layers.

[26] We observe a difference in x-ray intensity from the a_1 and a_2 domains, suggesting a preference for one type of domain over the other. Further investigations are under way to understand this result.

[27] K. Johnston, X. Huang, J. B. Neaton, and K. M. Rabe, Phys. Rev. B **71**, 100103(R) (2005).

[28] Y. L. Li, S. Y. Hu, D. Tenne, A. Soukiassian, D. G. Schlom, X. X. Xi, K. J. Choi, C. B. Eom, A. Saxena, T. Lookman, Q. X. Jia, and L. Q. Chen, Appl. Phys. Lett. **91**, 112914 (2007).

[29] E. Dooryhée, J. L. Hodeau, M. Nemoz, J. A. Rodriguez, C. Dubourdieu, R. Pantou, M. Rosina, F. Weiss, J. P. Sénateur, M. Audier, H. Roussel, and J. Lindner, J. Phys. IV **11**, Pr11-267 (2001).

[30] M. Nemoz, E. Dooryhée, J. L. Hodeau, C. Dubourdieu, H. Roussel, and P. Bayle-Guillemaud, J. Appl. Phys. **100**, 124110 (2006).

[31] R. J. Nelmes and A. Katrusiak, J. Phys. C **19**, L725 (1986).